Electrostatic forces in atomic force microscopy

B. M. Law[1] and F. Rieutord[2]
[1]*Condensed Matter Laboratory, Department of Physics, Kansas State University, Manhattan, KS 66506-2601*
[2]*Département de Recherche Fondamentale sur la Matière Condensée, Commissariat à l'Energie Atomique (CEA), 17 rue des Martyrs, 38054 Grenoble Cedex 9 France*
(Received 15 November 2001; published 26 June 2002)

In this paper we quantitatively compare various electrostatic models, which describe the interaction of a polarized atomic force microscopy tip with a molecularly smooth and grounded substrate, with a large experimental data set collected at many different tip potentials. The model by Hudlet *et al.* [Eur. Phys. J. B **2**, 5 (1998)] provides an excellent description of the experimental data for tip parameters (height H, cone half-angle θ_0, and tip radius R_0) close to their typical values, provided contributions from the cantilever body are included.

DOI: 10.1103/PhysRevB.66.035402 PACS number(s): 68.37.Ps, 07.79.Lh, 87.64.Dz

I. INTRODUCTION

The application of an electrostatic charge to the tip of an atomic force microscope (AFM) have found many uses. It has been used to (i) image small droplets situated upon a substrate on nanometer length scales,[1] (ii) study the charge mobility on ionic surfaces,[2] (iii) map the compositional pattern of buried organic interfaces,[3] and (iv) quantify the characteristics of charged surface sites.[4] Unfortunately, as is well known, a quantitative interpretation of the AFM signal is difficult because this signal invariably depends in a complicated fashion upon the tip shape and tip geometry. In fact, in the presence of electrostatic forces the cantilever (which is many microns from the surface under study) contributes a large background capacitance which gives rise to a background force on top of which charging effects at the tip must act. The major theoretical elements which describe the simplest and most well-studied geometry, of a conductive tip at constant potential approaching a grounded molecularly flat conductive surface, are now rather well understood. At small separation distances z between the tip and the substrate, the force of interaction is mainly influenced by the apex of the tip, which can be modeled by a sphere of radius R_0.[5] For $z \ll R_0$, the attractive interaction force reads

$$F \sim -R_0/z \tag{1}$$

which crosses over to

$$F \sim -(R_0/z)^2 \tag{2}$$

at somewhat larger distances. However at very large distances $R_0 \ll z \ll H$, but much less than the effective tip height H, the force of interaction is primarily influenced by the macroscopic tip geometry (Fig. 1) which can be modeled as a cone of height H and half-angle θ_0 at a constant potential V. Such an interaction can be represented by a line of charge of height H interacting with its image, thus giving[6]

$$F \sim \ln(z/H). \tag{3}$$

A rather complete discussion of the various theoretical models, together with a comparison with experiment, was provided in Ref. 7. Unfortunately these early models, as encompassed by the dependences exhibited in Eqs. (1)–(3), provide limited insight as to how the interaction force crosses over between the various force regimes. This difficult theoretical problem was recently approximately solved by Hudlet *et al.*[8] using an analytic scheme. They demonstrated that their theoretical formula [Eq. (5) below] provides reasonable agreement with experiment. However, the data set that they considered was rather sparse and consisted of just a few data points. Recent experimental work of Guggisberg *et al.*[9] found a rather unexpected behavior for the electrostatic interaction between an oscillating charged tip and a substrate, which differed considerably from the predictions of the Hudlet model. They attributed these differences to the presence of frozen charges on the tip, which were static over the oscillation cycle.

The purpose of this publication is to definitively check the validity of Eqs. (1)–(5) against a large data set collected at many different tip voltages. We find that a quantitative description of the experimental data can only be obtained using realistic tip parameters provided an additional cantilever contribution [Eq. (9)] is taken into account.

II. THEORY

The AFM tip and (triangular) AFM cantilever, which are both at a potential V, form a capacitor of complex geometry when in the vicinity of a grounded substrate. The force on the tip possesses the form

$$F = F_{bg} + \pi\varepsilon_0 (V - V_0)^2 f(z), \tag{4}$$

where F_{bg} represents any non-voltage-dependent background term originating from, for example, the van der Waals force, V_0 is a small residual surface potential (discussed below), and ε_0 is the vacuum permittivity, while $f(z) \sim dC/dz$ is generated by the variation in the capacitance C with separation distance z. The term $f(z)$ depends in a complicated fashion upon the geometric parameters R_0, θ_0, and H of the tip. By modeling the tip as a spherical apex and cone, Hudlet *et al.*[8] determined an approximate expression for the capacitance, and thus found the dimensionless electrostatic force $f(z)$. In their model[10]

 ©2002 The American Physical Society

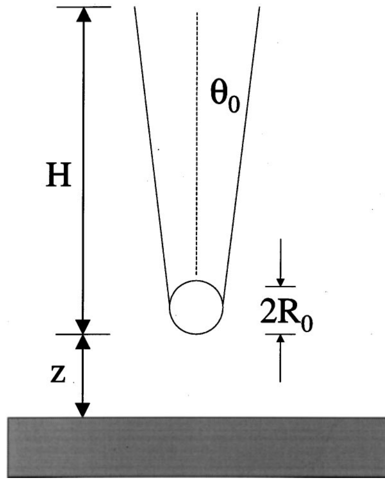

FIG. 1. Schematic diagram illustrating the AFM tip parameters.

$$f(z) = -K^2\left[\ln\left(\frac{H}{z+R_0(1-\sin\theta_0)}\right) - 1 + \frac{R_0\cos^2\theta_0/\sin\theta_0}{z+R_0(1-\sin\theta_0)}\right] - \frac{R_0^2(1-\sin\theta_0)}{z[z+R_0(1-\sin\theta_0)]} \tag{5}$$

with

$$K = 1/\ln[\tan(\theta_0/2)]. \tag{6}$$

This equation conforms with the limiting behaviors contained within Eqs. (1)–(3) and, additionally, provides an explicit prediction for the manner in which the interaction force crosses over between the various force regimes.

An alternative expression for $f(z)$ can be derived if the tip is modeled as a hyperboloid.[11,8] With the same parameters, the dimensionless force now reads

$$f(z) = -K^2\left[\ln\left(1+\frac{H}{z}\right) - \frac{\left(z-\frac{R_0}{\tan^2\theta_0}\right)H}{z(H+z)}\right]. \tag{7}$$

This expression is exact when the grounded plane and the conductive hyperboloid belong to the same set of equipotentials, namely, when

$$z = \frac{R_0}{\tan^2\theta_0}. \tag{8}$$

In both Eqs. (5) and (7), the contribution from the cantilever body is ignored. Although the cantilever body is located further away from the surface (at a distance larger than the tip height H), we show below that including this contribution is essential for obtaining correct values for the tip parameters. If the cantilever can be represented by a tilted electrode, with tilt angle α and a rectangular shape (width L_y, length L_x), then the force acting on the cantilever is

$$f_{\mathrm{lever}}(z) = \frac{1}{2\pi}\frac{L_xL_y}{(z+H)^2}\frac{1}{\left(1+\frac{L_x}{z+H}\tan\alpha\right)}. \tag{9}$$

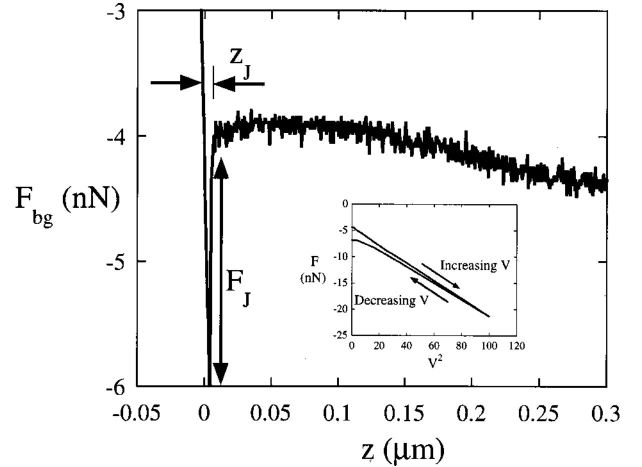

FIG. 2. The background F_{bg} between the AFM tip at 0 V and the grounded silane coated silicon wafer as a function of the distance from the surface at $z=0$. At large z, a repulsive force is present, indicating that some residual charges of the *same sign* exist on both the tip and the silicon wafer. At small z (within 0.05 μm of the surface), the force of interaction is attractive, most probably due to the attractive van der Waals interaction. In the inset we have plotted the force F as a function of V^2 at fixed $z \simeq 0.26\ \mu$m for both increasing and decreasing tip voltages. Residual charges are accumulating on the tip for decreasing voltage, as F is no longer linearly proportional to V^2.

The predictions contained within Eqs. (1)–(9) will be tested on many different levels in Sec. IV, from the global voltage dependence of F to the more microscopic details of $f(z)$, where the tip parameters play an essential role.

III. EXPERIMENTAL DETAILS

A Park Scientific AFM was used to collect force versus distance data at various dc tip voltages ranging from 0 to 10 V in 1 V steps. The AFM tip (Park Scientific Ultralever, ULCT) consisted of a silicon cantilever with silicon conical tip where $H \sim 6\ \mu$m, $\theta_0 \sim 12°$, a typical R_0 of a few tens of nanometers, and a typical force constant of $k = 0.26$ N/m. Two substrates were used. One was a bare silicon chip taken from the same material as the AFM cantilever itself. The second substrate consisted of a polished (100) silicon wafer, purchased from Semiconductor Processing Company, of thickness 3 mm and n-type phosphorous doping with a resistivity of 1–10 Ω cm. This wafer has a ~2-nm-thick oxide layer upon which we deposited an n-hexadecyltrichlorosilane self-assembled monolayer using a standard wet chemistry procedure.[12] After application of this silane coating, the outer surface consisted of an inert and homogeneous layer possessing methyl end groups ($-CH_3$) with low contact angle hysteresis (~1°–2° for n-octane droplets) and a surface roughness of ~0.5 nm over a 10×10-μm^2 area as measured by a contact mode AFM. This surface roughness conforms with the underlying surface roughness for a bare silicon wafer.[13] The results obtained from both substrates were similar.

The background force F_{bg}, as the tip approaches the surface at $z=0$ when the applied potential is 0 V, is shown in

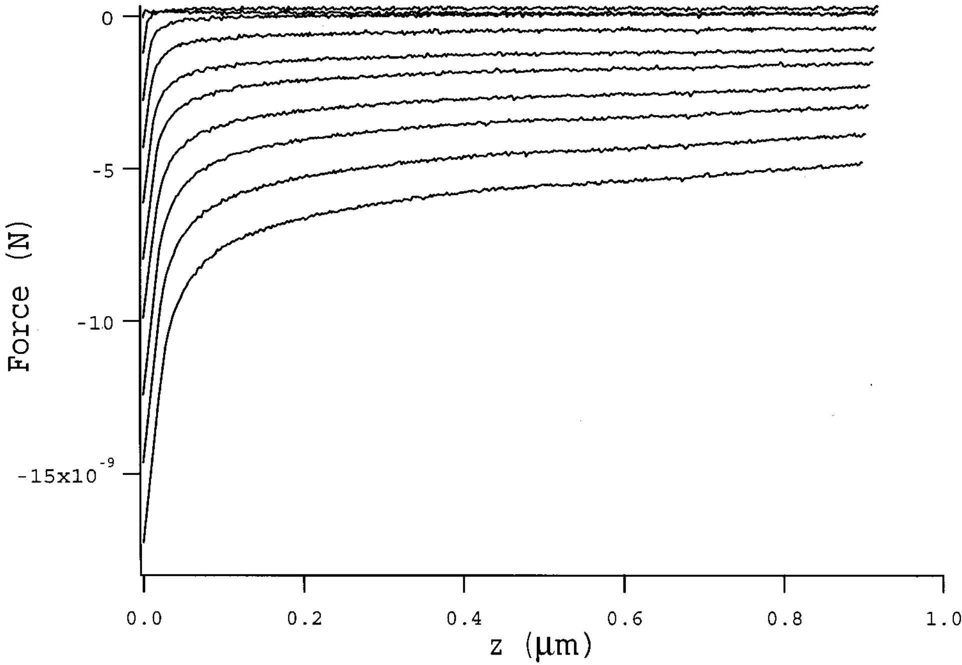

FIG. 3. The excess force $F-F_{\mathrm{bg}}$ plotted as a function of distance from the surface, at $z=0$, for various tip voltages from 1 to 10 V in 1 steps. (These data are from the "increasing" voltage data of Fig. 2 (inset) where no additional charge accumulates on the tip.)

Fig. 2. There are a number of important features that should be noted. The silicon wafer is grounded; therefore, under these conditions, one would normally only expect an *attractive* van der Waals force between the tip and the substrate. In fact, a large *repulsive* force is present at large distances and it is only when one is within 0.05 μm of the surface that an attractive force is evident. At a sufficiently small distance $z_J \approx 5.4$ nm, the tip jumps into contact with the surface when the attractive force overcomes the elastic restoring force of the cantilever; for the situation shown, the "jump-in" force $F_J \approx 1.8$ nN. The presence of the repulsive force implies that residual surface charges of the *same sign* reside on both the tip and the substrate. It is not surprising that these charges are present. It is well known that friction, when the tip and substrate make contact, can generate contact electrification[14] and, in fact, this effect has been observed before using an AFM.[4] These residual charges not only influence F_{bg} but also contribute a small surface potential V_0 which will be accounted for below. The term F_{bg} can be treated as an additive background and subtracted from F at *each* distance z. In the inset to Fig. 2 we show F as a function of V^2, at a fixed distance of $z \simeq 0.26$ μm, for both increasing and decreasing voltages. F scales with V^2 for increasing voltage and the force should be described by Eqs. (1)–(4). However, for decreasing voltage, the force no longer scales with V^2, and charge is accumulating on the tip. Hence, in the remainder of this paper, we will only consider the F versus z data collected during the "increasing voltage" stage.

IV. ANALYSIS

The normalized force $F-F_{\mathrm{bg}}$ as a function of the distance from the surface at $z=0$ (for different "increasing" voltages V) is depicted in Fig. 3. According to Eq. (4) the dimensionless force $f(z)=(F-F_{\mathrm{bg}})/\pi\varepsilon_0 V^2$ should fall on a *universal curve*, independent of V, provided that no residual potential acts between the tip and the surface. For sufficiently large values of V, the force scales with V^2 as expected, but deviations appear at low voltages. To account for the low voltage data, we have introduced a small surface potential $V_0(=0.52\ \mathrm{V})$ which is independent of z. The data can now be normalized to V^2-2VV_0 where the noise in the data for $f(z)$ decreases as the voltage V increases. Hence, the function $f(z)$ is better defined by the "high voltage" data, say 6–10 V (Fig. 4, symbols), and it will only be these data which will be used in the analysis of the shape of $f(z)$. The universal curve $f(z)$ contains information about the functional dependencies which are operative. In the following, we first demonstrate that the principal contributions at small and large z are described by Eqs. (1) and (3), respectively; we then consider the more complex and necessarily less illuminating "cross-over" forms described by Eqs. (5) and (7).

At large $z \gg R_0$, the dimensionless force reads

$$f(z) \approx f_1 + f_2 \ln(z), \tag{10}$$

according to Eqs. (3) and (5)–(7), where f_1 and f_2 are fitting parameters. This equation describes the data rather well [Fig. 4 (solid line) and Table I, column 1], except at very small z. A method for examining how well an equation fits the data, especially for equations which fit the data very well, is to plot the residuals

$$\mathrm{Re} = [f(z) - f_{fit}(z)]/\sigma \tag{11}$$

as a function of z where the standard deviation $\sigma = \sqrt{\chi^2/(N-\nu)}$, $\chi^2 = \Sigma_{i=1}^{N}[f_i(z) - f_{fit,i}(z)]^2$, $N(=2012)$ is the number of data points, while ν is the number of adjustable parameters. For a perfect fit, 67% of the points will fall between $\pm\sigma$, 95% of the points will fall between $\pm 2\sigma$, and all points will be randomly distributed about 0. The residuals in Fig. 4 indicate that the logarithmic fit in Eq. (10) is good at large z but it progressively worsens at small z. The height

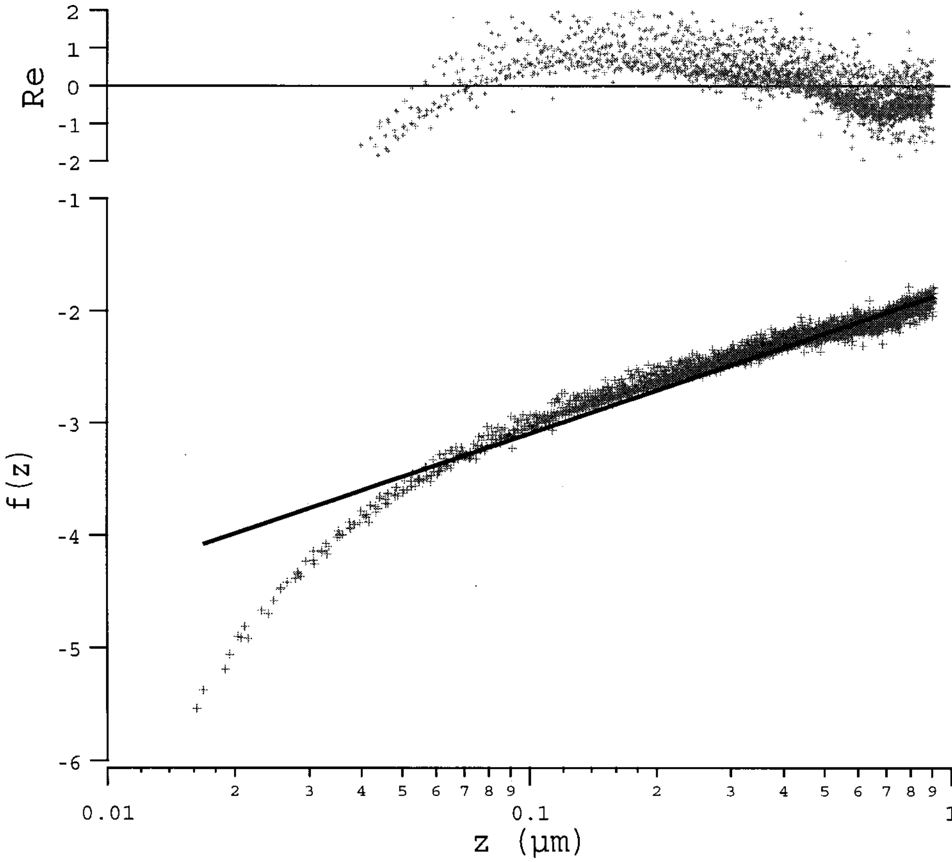

FIG. 4. Dimensionless force $f(z)$ calculated from the 6–10 V data in Fig. 3 using Eq. (4). All of the data fall on the same universal scaling curve where the shape of $f(z)$ is better defined the higher the voltage V. The solid line represents a fit to the $f(z)$ data using Eq. (10), where the fitting parameters are listed in Table I, column 1. The residuals Re indicates that the fit is good at large z but progressively worsens at very small z.

H and cone half-angle θ_0 can be calculated from f_1 and f_2 (Table I, column 1) by Taylor expanding Eq. (5) or (7) together with Eq. (6), from which

$$f_1 = -K^2(\ln H - 1), \tag{12}$$

$$f_2 = K^2. \tag{13}$$

The data values for both $H(=73\ \mu\text{m})$ and $\theta_0(=29.2°)$ obtained from these equations are considerably above the typical specifications of 6 μm and $\sim 12°$.

The deviations observed in Fig. 4, at small z, can be approximately accounted for by including a z^{-1} term. Thus

$$f(z) \approx f_1 + f_2 \ln(z) + f_3/z \tag{14}$$

should provide a better description of the data where $f_3 \propto -R_0$. This equation (Fig. 5, solid line) describes the data (symbols) very well where the residuals are more uniformly distributed about 0 compared with Fig. 4. The additional tip parameter R_0 can be calculated from f_3. However, the Taylor expansions of Eqs. (5) and (7), for $z \ll R_0$, are different for the two models:

$$f_3 = -K^2 \frac{R_0}{\tan\frac{\theta_0}{2}} \quad \text{for Eq. (5)}, \tag{15}$$

$$f_3 = -K^2 \frac{R_0}{\tan^2 \theta_0} \quad \text{for Eq. (7)}. \tag{16}$$

TABLE I. Fitting parameters.

Column	1	2	3	4	5	6
Eq.	(10)	(14)	(5)	(7)	(5)+(9)	(7)+(9)
f_1	-1.822 ± 0.004	-1.891 ± 0.002				
f_2	0.554 ± 0.003	0.341 ± 0.003				
f_3 (nm)		-34.6 ± 0.4				
θ_0	29.2°	20.5°	$21.5 \pm 0.1°$	$20.5 \pm 0.1°$	$13.3 \pm 0.2°$	$14.9 \pm 0.3°$
H (μm)	73	692	503 ± 20	687 ± 34	5.97 ± 0.02	6.29 ± 0.03
R_0 (nm)		18.4 [Eq. (5)] 14.3 [Eq. (7)]	42.5 ± 0.4	14.1 ± 0.1	47.9 ± 0.3	11.7 ± 0.1
χ^2	28.3	6.05	5.94	6.05	5.99	5.80

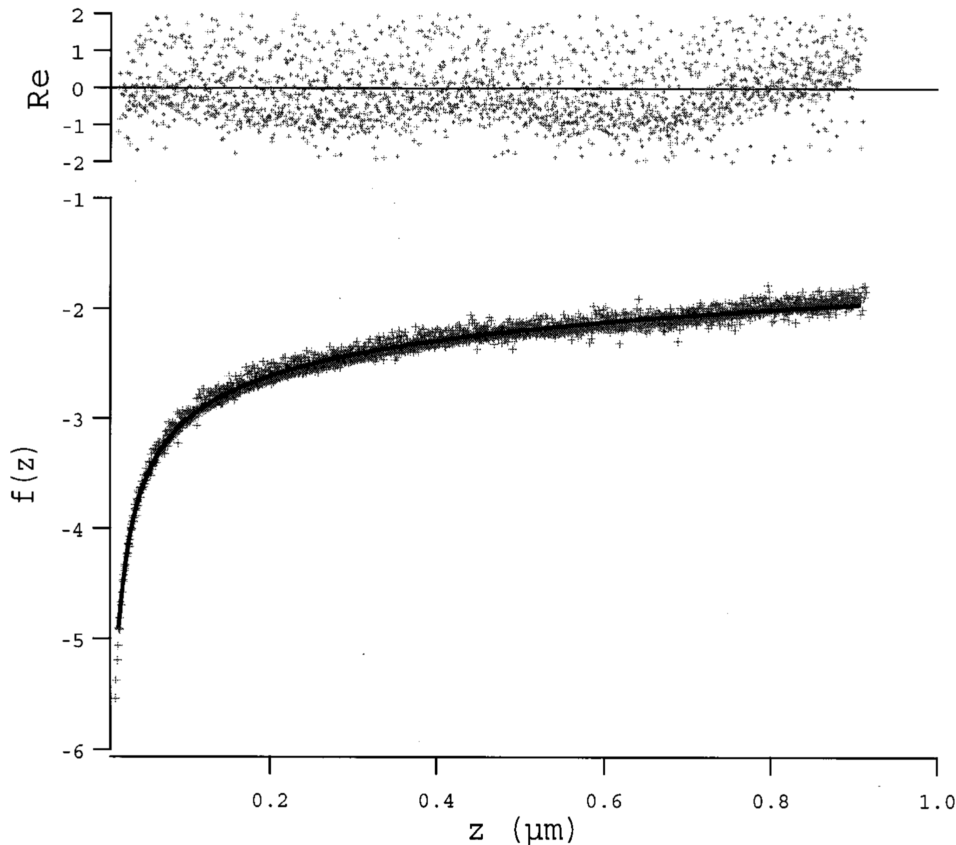

FIG. 5. Comparison of the 6–10 V $f(z)$ data with Eq. (14) where the fitting parameters are listed in Table I, column 2. The residuals Re are reasonably randomly distributed about zero.

The values obtained for H and θ_0 (Table I, column 2) are, however, again considerably above the tip specifications.

We now use the full equations (5) and (7), with the same number (3) of parameters, namely, R_0, θ_0, and H to model the data. As is evident from Table I (columns 3 and 4), the fit quality remains very good ($\chi^2 \approx 6$) using these full-fledged equations; however the values for $\theta_0(\simeq 21°)$ and H ($\simeq 600\ \mu$m) still remain considerably above specifications ($\sim 12°$ and 6 μm). The residuals (which are not plotted) do not exhibit a significant improvement over and above the residual plot displayed in Fig. 5. The anomalously high values for θ_0 and H indicate that something is still missing from our model of the electrostatic interaction.

Let us finally consider the cantilever contribution, namely, Eq. (9) added to Eq. (7) or (5). It can be seen from the Taylor expansion of this additional term, that, when $z \ll H \ll L_x = 180\ \mu$m, the lever contribution to the force is essentially a constant (with respect to the tip-surface distance z) dependent upon the fitting parameter H, but independent of the cantilever length. The other parameters, entering this contribution, are known and are kept fixed at $\alpha = 15°$ and $L_y = 25\ \mu$m. Columns 5 and 6 in Table I demonstrate that when this contribution is added, the fit quality remains very good ($\chi^2 \approx 6$), where in addition the parameters θ_0 ($\sim 14°$) and H ($\sim 6\ \mu$m) now fall within the expected specifications. Thus a combination of either the Hudlet model [Eq. (5)] or the hyperboloid model [Eq. (7)] together with the cantilever contribution [Eq. (9)] provides an excellent quantitative description of the experimental data with realistic values for these tip parameters.

However, there remains a difference between the Hudlet and hyperboloid models which needs to be discussed. For the former model the radius of curvature of the tip is $R_0 \simeq 48$ nm, while for the latter it is $R_0 \simeq 12$ nm. The reason for this difference can be readily understood when the two profiles are superimposed upon each other for the same parameter values [Fig. 6(a)]. The hyperboloid goes gradually from a radius $R = R_0$ at the tip end to $R = \infty$ far from the tip; hence the amount of material present in the neighborhood of the opposing surface is much higher for the hyperboloid (light line) than for the sphere/cone of Hudlet (dark line), which appears to be much sharper. Thus, for the electrostatic force, this difference in shape is compensated by choosing a larger radius of curvature for the Hudlet model [Eq. (5)], compared with the hyperboloid model [Eq. (7)]. This is illustrated in Fig. 6(b), where the two profiles with the best fit parameters are displayed—the overall shape of the two curves is remarkably similar. Contact mode AFM images of the tip, against a scanning probe microscope grating sample possessing very sharp edges, exhibit profiles very close to what is shown in this figure, thus giving a final validation to our electrostatic procedure.

V. SUMMARY

In this publication, we have found that provided a background term $F_{\rm bg}$ at 0 V is subtracted and the surface potential term V_0 is accounted for, the dimensionless electrostatic force $f(z) = (F - F_{\rm bg})/\pi\varepsilon_0(V - V_0)^2$ can be described by a universal curve (Fig. 4, symbols). The dominant features of

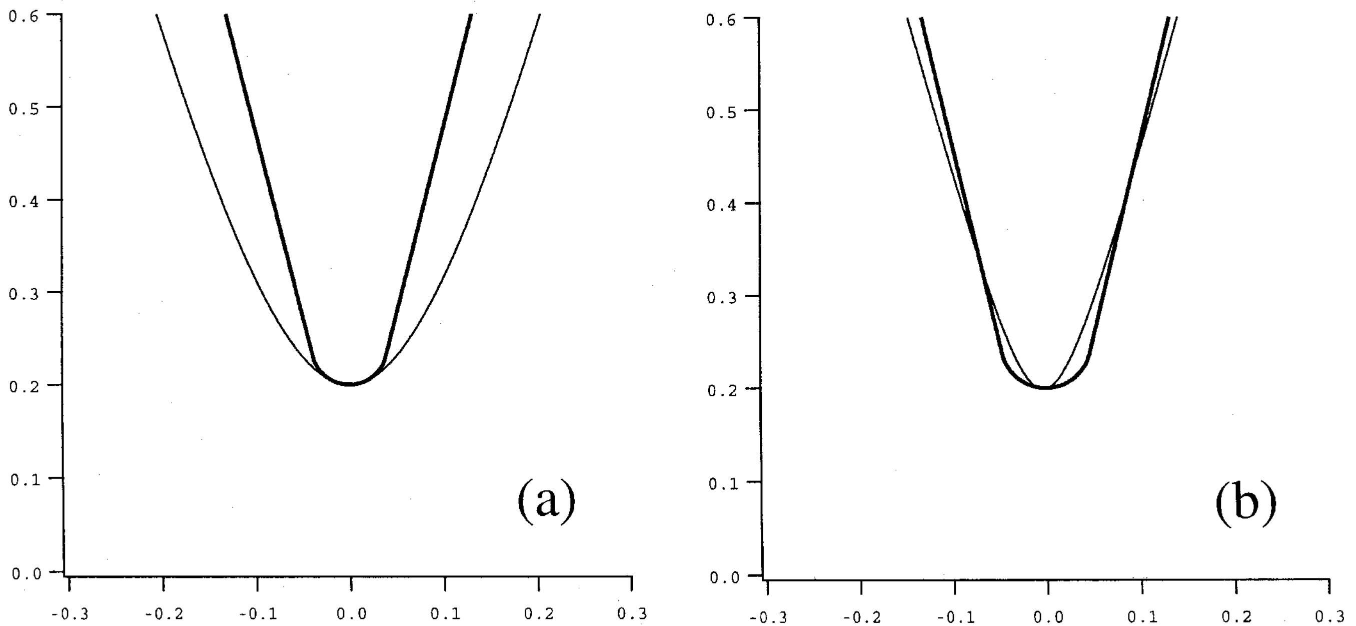

FIG. 6. Comparison of the hyperboloid tip (light line) and the cone/sphere tip (dark line) for, respectively, (a) identical tip parameters and (b) the best-fit parameters.

this universal curve are described by a $\ln z$ and z^{-1} dependence at, respectively, large z (Fig. 4) and small z (Fig. 5) where the crossover between these two asymptotic behaviors is correctly described by Eq. (5) or (7) (Table I, columns 3 and 4). We have shown that the tip parameters θ_0, H, and R_0 can be reliably derived from a fit to the $f(z)$ data provided that the contribution from the cantilever body [Eq. (9)] is included. The most amazing and interesting part of these results is that one can obtain geometric information on three microscopic (and even nanoscopic) parameters of an AFM tip (its radius of curvature, the opening angle of the tip, and its height) without the use of any microscopic imaging technique (e.g., AFM, TEM, etc.).

ACKNOWLEDGMENTS

B.M.L. would like to thank colleagues at CEA, DRFMC, Grenoble for their kind hospitality and for financial support through Université Joseph Fourier during his stay in Grenoble. B.M.L. also acknowledges partial support for this work under NSF Grant No. DMR-0097119.

[1] J. Hu, X.-D. Xiao, and M. Salmeron, Appl. Phys. Lett. **67**, 476 (1995); M. Salmeron, L. Xu, J. Hu, and Q. Dai, MRS Bull. **22**, 36 (1997); F. Rieutord and M. Salmeron, J. Phys. Chem. B **102**, 3941 (1998).

[2] M. Luna, F. Rieutord, N. A. Melman, Q. Dai, and M. Salmeron, J. Phys. Chem. A **102**, 6793 (1998).

[3] H. Takano, S.-S. Wong, J. A. Harnisch, and M. D. Porter, Langmuir **16**, 5231 (2000).

[4] M. Saint Jean, S. Hudlet, C. Guthmann, and J. Berger, Eur. Phys. J. B **12**, 471 (1999).

[5] R. Erlandsson, G. M. McClelland, C. M. Mate, and S. Chiang, J. Vac. Sci. Technol. A **6**, 266 (1988); C. Schönenberger and S. F. Alvarado, Rev. Sci. Instrum. **60**, 3131 (1989); B. D. Terris, J. E. Stern, D. Rugar, and H. J. Mamin, Phys. Rev. Lett. **63**, 2669 (1989); Y. Martin, D. W. Abraham, and H. K. Wickramasinghe, Appl. Phys. Lett. **52**, 1103 (1988).

[6] H. W. Hao, A. M. Baró and J. J. Sáenz, J. Vac. Sci. Technol. B **9**, 1323 (1991); H. Yokoyama, T. Inoue, and J. Itoh, Appl. Phys. Lett. **65**, 3143 (1994).

[7] S. Belaidi, P. Girard, and G. Leveque, J. Appl. Phys. **81**, 1023 (1997).

[8] S. Hudlet, M. Saint Jean, C. Guthmann, and J. Berger, Eur. Phys. J. B **2**, 5 (1998).

[9] M. Guggisberg, M. Bammerlin, Ch. Loppacher, O. Pfeiffer, A. Abdurixit, V. Barwich, R. Bennewitz, A. Baratoff, E. Meyer, and H.-J. Güntherodt, Phys. Rev. B **61**, 11 151 (2000).

[10] We take $F<0$ for an attractive force. However, Eq. (5) differs by a negative sign in front of the Ln term, compared with the corresponding formula given in Ref. 8 due to a sign error. Our expression is in agreement with their Eq. (9), and their discussion.

[11] E. Durand, *Électrostatique et Magnétostatique* (Masson, Paris, 1953).

[12] J. B. Brzoska, I. Ben Azouz, and F. Rondelez, Langmuir **10**, 4367 (1994).

[13] J. Y. Wang, S. Betelu, and B. M. Law, Phys. Rev. Lett. **83**, 3677 (1999); J. Y. Wang, S. Betelu, and B. M. Law, Phys. Rev. E **63**, 031601 (2001).

[14] W. R. Harper, *Contact and Frictional Electrification* (Oxford University Press, London, 1967).